DEVELOPMENT AND PARAMETER ESTIMATION OF A COMPACT ELECTRONIC WEDGE BRAKE TEST RIG USING GREY BOX SYSTEM IDENTIFICATION

M.H. Che Hasan[1], M.K. Hassan[2], F. Ahmad[3], M.H. Marhaban[2] and S.I. Haris[4]

[1]Faculty of Electrical and Electronic Engineering Technology,
[3]Faculty of Mechanical Engineering,
Universiti Teknikal Malaysia Melaka, Durian Tunggal, 76100, Melaka, Malaysia.

[2]Faculty of Engineering, Universiti Putra Malaysia, Serdang, 43400, Selangor, Malaysia.

[4]Kolej Kemahiran Tinggi MARA, Masjid Tanah, 78300 Melaka

Corresponding Author's Email: [1]hanif.hasan@utem.edu.my

ABSTRACT: *This article presented the development and model parameter estimation of a compact electronic wedge brake (EWB) test through mathematical modelling and system identification (SI). The EWB test rig was vast and complex, leading to high costs and time consumption. Additionally, the EWB parameters estimation was limitedly discussed. Thus, a compact test rig was developed to produce up to 300N of braking force, which was acceptable to demonstrate the effectiveness of the model and EWB performance. Two separate transfer function models for the motor and EWB mechanism were proposed. The parameter estimation was made using the grey box approach, which combined mathematical modelling and SI. The complete physical parameters value via two separated SI was successfully obtained. The brake responses were analysed by comparing the simulation and experiment under rapid control prototyping (RCP). The average percentage of root mean square error (RMSE) value between the simulation and experiment was less than 6.23%. The test rig configuration and proposed model guarantees were helpful in preparing a simpler, low-cost brake test rig and provided an alternative way to obtain model physical parameter values.*

KEYWORDS: *Modelling; Electronic Wedge Brake (EWB); System identification (SI); Rapid Control Prototyping (RCP); Root Mean Square Error (RMSE).*

1.0 INTRODUCTION

The Brake by Wire (BBW) is a modern brake system that completely replaces the traditional brake mechanism. The Electro-Mechanical Brake (EMB) uses electronically powered actuators to generate braking force. Its benefits include noiseless operation, quicker response time, ease of control system creation, and incredible environmental friendliness.[1]. Most EMBs have an electric motor, a reduction gear, a floating disc brake calliper, and a 24/42-volt power supply [2], [3] and consume much energy [4]. The EWB is from the EMB category that, by employing the self-reinforcement principle, can reduce energy usage. The EWB technology has been a popular alternative because it can run at a minimum voltage and uses around one-tenth of the power [5].

Model-based approaches, prevalent in modern control strategies, benefit significantly from representation in state space and transfer function representation. Modern control strategies applied on EWB so far, such as PID [6], Linear Quadratic Regulator (LQR) [7], Sliding Mode Control (SMC) [8], and Youla parameterisation [9], are highly dependent on a model. However, finding all the EWB parameters must first be found to design a suitable controller. The SI is often used to find model parameters. Part of SI, the grey box approach, combines the benefits of white and black box testing. The white box approach has been used for EWB in several studies. The approach is applied by [10], where a state-space representation of the EWB model is used to construct a braking force controller. The EWB model is created using ordinary differential equations (ODE) and is divided into three sub-assemblies: the DC motor, lead screw, and EWB brake heart. As the study continues, additional mathematical models of the EWB system are being developed [8], [11]–[17]. Meanwhile, the black box approach is also used. The EWB mechanism model is experimentally obtained as a second-order transfer function via the black-box approach [18]. Besides, the wedge disk brake empirical model is constructed based on the Box-Behnken design [19]. A series of experiments are conducted to evaluate the performance of EWB. As discussed in [20]–[22], the performance based on different actuation angles is analysed using analytical and experimental approaches.

This research aims to develop a small and affordable brake test rig that can demonstrate and analyse the EWB, as most experimental conduct uses expensive and complex large-scale test rigs. The literature shows limited discussion on the EWB model and its relationship with SI, with only one research paper attempting to

model the wedge mechanism through a black-box approach [18]. Based on the author's knowledge, there is no further research on using the grey box approach to estimate physical parameters. This study offers a simpler and cost-effective alternative for obtaining model physical parameter values.

There are four sections in this article. The first part discusses the EWB-relevant work conducted by researchers. The second section explains the methodology used for EWB modelling, which focuses on two separate models proposed for SI. The compact brake test rig setup, which consists of all hardware used, configuration, and wiring, is also presented. In the third section, the EWB brake response and its performance are compared and validated between simulation and experimentation. The model's accuracy is measured using the root means square error (RMSE), and the article concludes with a final section.

2.0   METHODOLOGY

The study utilised a 5th-order linear model that was previously introduced [23]. The model had two mechanisms, the motor and the wedge, each with a transfer function. A grey-box approach was used to get the necessary parameters. To validate the model, a compact brake test rig was developed.

2.1   Modelling

The EWB mechanism output was the clamping force (F_c) which is dependent on clipper stiffness (K_{cal}), wedge deflection (X_w), and wedge angle (α), as described as follows.

$$F_c = K_{cal} X_w \tan \alpha \qquad (1)$$

In the meantime, a wedge mechanism dynamic of the wedge brake is described as

$$\dot{V}_w = \left[\frac{K_{cal} \tan \alpha \, (\mu - \tan \alpha)}{M_w (\tan^2 \alpha + 1)} \right] X_w + \left[\frac{1}{M_w (\tan^2 \alpha + 1) \cos \beta} \right] F_m \qquad (2)$$

Where:

$$\beta = \begin{cases} 0 & , for\ Tangential\ Inclination \\ \alpha & , for\ Best\ Inclination \end{cases}$$

In equation (2), the wedge velocity, brake pad coefficient, wedge

mass, and motor force were denoted as V_w, μ, M_w and F_m respectively. The transfer function for equation (2) can be stated as

$$\frac{X_w(s)}{F_m(s)} = \frac{1}{a_1 a_3 s^2 + a_2 a_3} \tag{3}$$

Where

$$a_1 = M_w(tan^2\,\alpha + 1)$$
$$a_2 = K_{cal}\,tan\,\alpha\,(tan\,\alpha - \mu)$$
$$a_3 = cos\,\beta\,, \beta = \begin{cases} 0 & ,for\;Tangential\;Inclination \\ \alpha & ,for\;Best\;Inclination \end{cases}$$

The motor force was obtained from motor torque (lead screw torque) which was connected through a lead screw. This relationship was described in the frequency domain as

$$F_m = L_a N_a \frac{(D_a s + K_a)}{2\pi}\theta_m - \frac{(D_a s + K_a)}{cos\,\beta}X_w \tag{4}$$

The equation (1), (3) and (4) could be combined to get a single transfer function for the EWB mechanism as

$$G_{wedge}(s) = \frac{F_c}{\theta_m} = \frac{a_3 a_4 (D_a s + K_a) K_{cal}\,tan\,\alpha}{a_1 a_3{}^2 s^2 + D_a s + a_2 a_3{}^2 + K_a} \tag{5}$$

Where

$$a_4 = \frac{L_a N_a}{2\pi}$$

The equation (5) describes the system as second order with two poles and a system type of 1, indicating a single zero. This aligns with the transfer function obtained through the black-box approach in EWB [18]. However, the experimenters were unable to locate the zero of the system due to the low axial damping value. Figure 1 presents the PMDC and EWB mechanism models proposed.
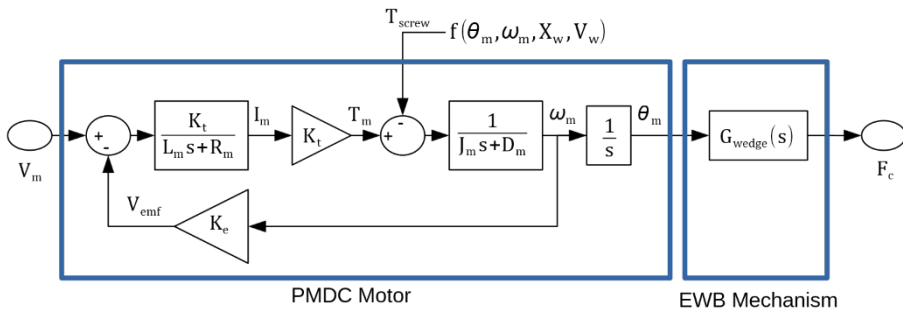
Figure 1: Overall EWB frequency-based block diagram

2.2 System Identification

The PMDC motor's parameters were estimated using available data and physical evaluation. Four parameters were obtained from datasheet while two others were determined by solving the transfer function model from SI. The SI was performed based on the transfer function with the number of poles and zero set to 3 and 0, respectively. During the experiment, the EWB mechanism was disconnected from the motor. The best transfer function has a curve fit of 94.2% and has a minimum noise spectrum. It was as follow:

$$G_{motor\_exp}(s) = \frac{\theta_m}{V_m} = \frac{9551.4}{s(s^2 + 21.34s + 158.3)} \qquad (6)$$

Meanwhile, the EWB mechanism could be directly observed by the second order with type 1 system transfer function as described in equation (5). There were four parameter values to estimate, which were the wedge mass (M_w), brake calliper stiffness (K_{cal}), lead screw viscous damping (D_a) and lead screw stiffness (K_a).

The average best fit for the model was 76.88%, with distortion occurred at a low level of brake amount. The best transfer function has a curve fit of 90.6% at highest brake magnitude and has a minimum noise spectrum. The approximated transfer function was as follow:

$$G_{wedge\_exp}(s) = \frac{F_c}{\theta_m} = \frac{0.0497s + 6.4736e + 11}{s^2 + 1.9175e - 04s + 2.5060e + 09} \qquad (7)$$

Based on these two separated SI, the parameters are obtained as presented in [23].

2.3 Experimental Setup

The RCP implementation is a fundamental step in model validation via experiment. The brake test rig had been constructed with a single car wheel, calliper, EWB brake, flywheel, and 3-phase motor. The EWB brake was controlled by computer, and sensors data was recorded during braking tests using the Simulink desktop real-time. Figures 2 show the wiring connection for the EWB based test rig system.
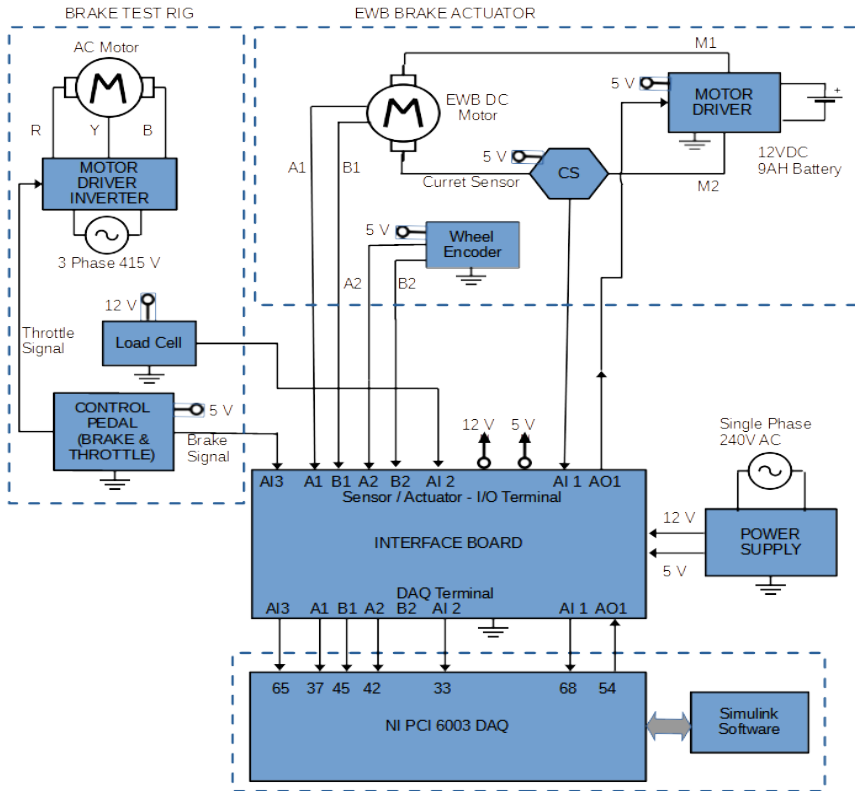
Figure 2: The EWB experimental wiring connection

The accelerator pedal was connected to the motor inverter, allowing for adjustment of the wheel speed. The EWB DC motor was supplied with adequate current as needed by the 12V lead-acid battery. A compact brake test rig was created to test the efficiency and functionality of the EWB, though it was only capable of testing brake effectiveness at a low level. Table 1 shows the specifications of the brake test rig.

Table 1: Brake test rig specification

	Item	Specification
1	Motor	IEC, 3phase Asynchronous Motor MS802-4, 1HP
2	Motor Inverter	Rexroth variable frequency drive, FSCS01
3	Wheel Speed Sensor	Encoder TR1 TRU-TRAC.
4	Brake Force Sensor	Futec LCF451, FSH04300 with CSG110 Amplifier.
5	Flywheel Rotational Inertia	2.9760 Kg m2
6	Permissible Braking Torque	36 Nm
7	Maximum Rotation Speed	390 RPM
8	Disk Brake Effective Radius, Rc	0.12 m

3.0   RESULTS AND DISCUSSION

The validation of the model with the EWB prototype was performed based on parameters obtained. The validation consists of 2 parts: EWB brake force performance and test rig implementation.

3.1   EWB Brake Force Performance

A single-loop P controller was used for motor position control. Three brake levels were used. The brake test lasted 5 seconds, with brakes applied from 2 to 2.1 seconds and then released from 3.9 seconds. Figures 3(a) and 3(b) illustrate the control target and actual response (wedge angular position) of EWB and its corresponding brake force.

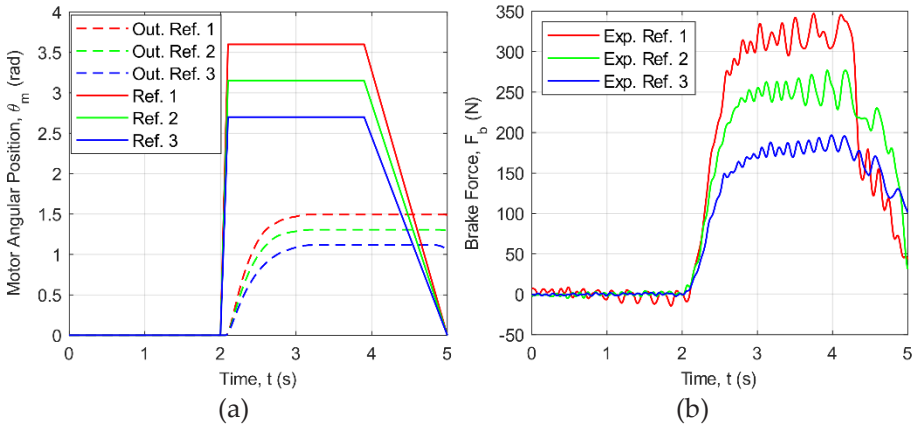(a)   (b)

Figure 3: EWB prototype responses (a) Control target and actual (b) Brake force

The experiment showed a response time of 0.51, 0.53, and 0.63 seconds for the 1st, 2nd, and 3rd magnitudes. The brake force was proportional to the motor position and had periodic noise that interfered with the load cell reading. The maximum brake force suddenly decreased when the wheel speed reached zero. The experiment observed and compared the motor position, voltage, and brake force with the simulation as in Figure 4 until Figure 6. Motor position varied during clamping but returned to the initial position slower than simulation. Steady-state showed minimal error. Figure 5 shows the motor voltage and its error. While releasing the brake, the motor voltage used in the experiment was slightly lower than in the simulation. This could be attributed to the fact that the system dynamic used for this research only accounted for clamping. The brake force and its error were plotted in Figure 6(a) and Figure 6(b), respectively.
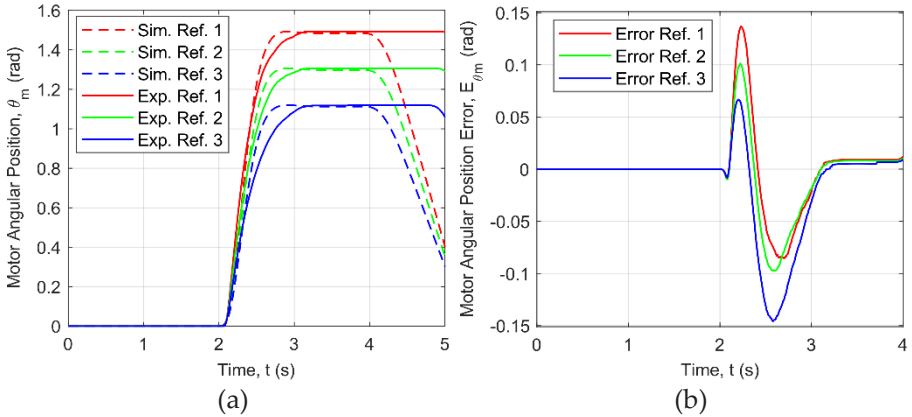
Figure 4: Motor angular position - simulation vs experimental (a) Response (b) Response error
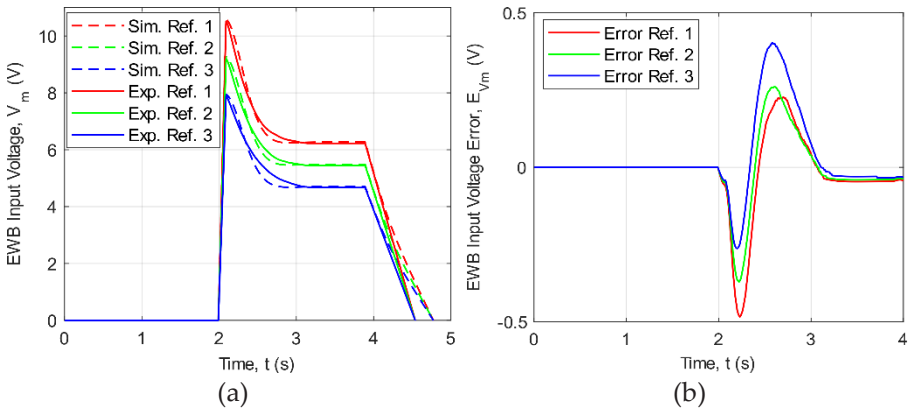

Figure 5: Motor voltage - simulation vs experimental (a) Response (b) Response error
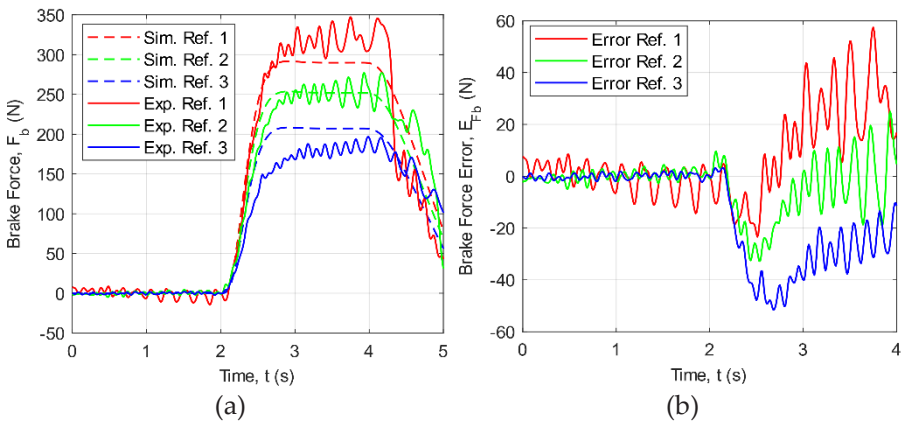

Figure 6: Brake force - simulation vs experimental (a) Response (b) Response error

The error between simulation and experimental results was measured using the RMSE value summarised in Table 2. Here, it can be seen that the minimal errors for motor input voltage and position, but braking force had the highest error at 11.26%. The highest brake force tested had an error of 17.36% due to vibration, causing the highest error for each response measured.

Table 2: RMSE between simulation and experimental

Response error	Brake 1	Brake 2	Brake 3	Average
Motor Position Error, $E\theta m$ (rad)	0.0356 (3.84%)	0.0323 (3.98%)	0.0438 (6.29%)	0.0372 (4.71%)
Motor Input Voltage Error, EVm (V)	0.1166 (2.38%)	0.1006 (2.35%)	0.1251 (3.41%)	0.1141 (2.71%)
Brake Force Error, EFb (N)	17.5148 (9.67%)	10.6526 (6.76%)	22.4729 (17.36%)	16.8801 (11.26%)

3.2 Brake Test Rig Implementation

The braking system was evaluated by observing the wheel speed during braking at three different levels with an initial wheel speed of 390 RPM. Figure 7(a) shows this was done at the 2-second timeline. As anticipated, the speed of the wheel decreased in proportion to the brake applied. However, there were inconsistencies between the simulation and the actual results, particularly for the first and third brake levels. This was due to the nonlinear relationship between the brake force and the motor angle as highlighted in [24]. Figure 7(b) displays the results of tests conducted on braking equipment at various initial wheel speeds. A single brake level was used with a brake force of 262.4 N. The wheel speed slows down by 20 rad/s^2 and stops completely after 3 seconds.
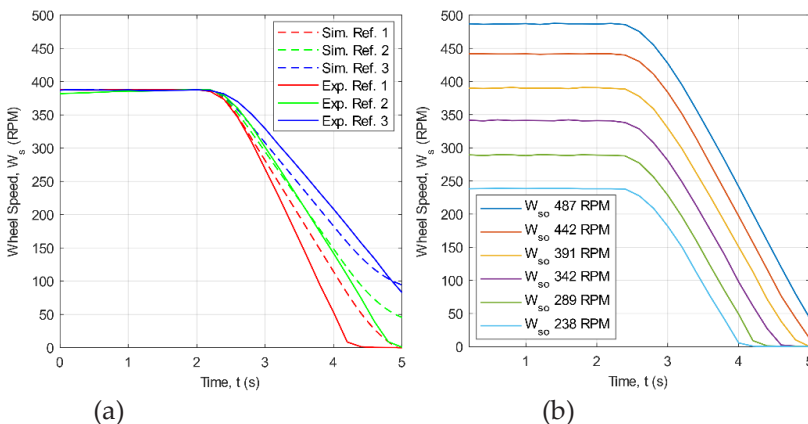

(a) (b)

Figure 7: Wheel speed of test rig - simulation vs experimental (a) Different braking level (b) Different wheel speed

4.0 CONCLUSION

The EWB test rig developed is a simple, cost-effective solution with a short development time. However, it has limited capabilities, as it can test the brake up to 300N only. The proposed separated transfer function for the motor and EWB mechanisms has enabled grey box SI, allowing accurate estimation of all physical parameters instead of just obtaining the transfer function coefficient in the black box model approach. With an average RMSE percentage of 6.23%, the accuracy of the theoretical part discussed is valid and acceptable. The brake response for six different speeds of the wheel has demonstrated that the EWB performance is consistent. It has been found through experimentation that there are different responses between the experiment and simulation for brake release, which demonstrates that the proposed model is valid only for clamping mode behaviour. Furthermore, the nonlinear behaviour of brake pad and clipper stiffness has been detected, which be useful for future research work.

ACKNOWLEDGMENTS

REFERENCES

[1]   W. A. S. P. Abeysiriwardhana and A. M. H. S. Abeykoon, "Brake by wire control with pedal feedback and brake boost," *Bulletin of Electrical Engineering and Informatics*, vol. 10, no. 6, pp. 3042–3051, Dec. 2021.

[2]   H. Hartmann, M. Schautt, A. Pascucci, and B. Gombert, "eBrake ® – The Mechatronic Wedge Brake," *SAE Technical Paper*, pp. 2002-01–2582, 2002.

[3]   C. Li *et al.*, "A Review of Electro-Mechanical Brake (EMB) System: Structure, Control and Application," *Sustainability (Switzerland)*, vol. 15, no. 5, Mar. 2023, doi: 10.3390/su15054514.

[4]   B. D. M. Gombert, M. Schautt, and R. P. Roberts, "The Development of Alternative Brake Systems," in *Encyclopedia of Automotive Engineering*, Chichester, UK: John Wiley & Sons, Ltd, 2014, pp. 1–11.

[5]   K. Han, K. Huh, M. Kim, W. Hwang, and D. Kim, "EWB Control

Based on the Estimated Clamping Force," in *SAE Technical Paper*, Sep. 2012, pp. 2012-01–1797.

[6] S. I. Haris, F. Ahmad, M. H. Che Hasan, and A. K. Mat Yamin, "The Experimental Evaluation of Cone Wedge Shape based Electronic Wedge Brake Mechanism in Vehicle Braking System," *Automotive Experiences*, vol. 5, no. 3, pp. 433–451, Sep. 2022.

[7] M. S. Jneid and A. Joukhadar, "LQR-Based Control of a Single Motor Electronic Wedge Brake EWB for Automotive Brake-By-Wire System," *Soft Computing and Electrical Engineering*, vol. 1, no. 1, pp. 12–35, 2019.

[8] F. Xu and C. Cho, "A Novel Electronic Wedge Brake Based on Active Disturbance Rejection Control," *Energies (Basel)*, vol. 15, no. 14, p. 5096, Jul. 2022.

[9] E. Arasteh and F. Assadian, "A Comparative Analysis of Brake-by-Wire Smart Actuators Using Optimization Strategies," *Energies (Basel)*, vol. 15, no. 624, pp. 1–22, Jan. 2022.

[10] J. Fox, R. Roberts, C. Baier-Welt, L. M. Ho, L. Lacraru, and B. Gombert, "Modeling and Control of a Single Motor Electronic Wedge Brake," *SAE Technical Paper*, pp. 2007-01–0866, 2007.

[11] C. Jo, S. Hwang, and H. Kim, "Clamping-force control for electromechanical brake," *IEEE Trans Veh Technol*, vol. 59, no. 7, pp. 3205–3212, 2010.

[12] M. A. A. Emam, A. S. Emam, S. M. El-Demerdash, S. M. Shaban, and M. A. Mahmoud, "Performance of Automotive Self Reinforcement Brake System," *Journal of Mechanical Engineering*, vol. 1, no. 1, pp. 4–10, 2012.

[13] A. Ghajari and R. Kazemi, "A New Approach to the Electronic Wedge Brake," *SAE Technical Paper*, pp. 2012-01–1801, 2012.

[14] K. Han, K. Huh, and M. Kim, "Modeling and control of an electronic wedge brake," *Proc Inst Mech Eng C J Mech Eng Sci*, vol. 226, no. 10, pp. 2440–2455, Oct. 2012.

[15] M. S. Jneid, M. Zöldy, and P. Harth, "Sensorless optimal control of electronic wedge brake based on dynamic model and Kalman filter state multiple-estimation," *Proceedings of the Institution of Mechanical*

Engineers, Part D: Journal of Automobile Engineering, p. 095440702311681, Apr. 2023, doi: 10.1177/09544070231168168.

[16] E. Arasteh and F. Assadian, "Bond Graph Modeling of Brake-By-Wire Actuators on a One-Wheel Vehicle Model," in *Simulation Series*, G. J. J. Karnopp D.C., Ed., The Society for Modeling and Simulation International, 2021, pp. 169–178.

[17] M. Yao, J. Miao, S. Cao, S. Chen, and H. Chai, "The Structure Design and Optimization of Electromagnetic-Mechanical Wedge Brake System," *IEEE Access*, vol. 8, pp. 3996–4004, 2020.

[18] F. Ahmad *et al.*, "Modelling and control of a fixed calliper-based electronic wedge brake," *Journal of Mechanical Engineering*, vol. 63, no. 3, pp. 181–190, 2017.

[19] N. M. Ghazaly, M. M. Makrahy, K. A. A. E. Gwwad, K. R. Mahmoud, and A. M. A. E. Tawwab, "Experimental Evaluation of an Empirical Model for Wedge Disc Brake using Box-Behnken Design," *International Journal of Vehicle Structures and Systems*, vol. 6, no. 3, pp. 58–63, Aug. 2014.

[20] D. H. Shin *et al.*, "Analytic approaches for keeping high braking efficiency and clamping efficiency of electro wedge brakes," *International Journal of Precision Engineering and Manufacturing*, vol. 16, no. 7, pp. 1609–1615, 2015.

[21] J. Wang, Y. Zhang, N. Yang, D. Song, and Q. Wang, "Parameters design and braking efficiency analysis of a hydraulic self-energizing wedge disc brake," *International Journal of Precision Engineering and Manufacturing*, vol. 18, no. 10, pp. 1409–1418, 2017.

[22] K. R. M. Mahmoud, M. M. Makrahy, K. A. A. El Gwwad, N. M. Ghazaly, and A. M. A. El Tawwab, "Effect of wedge inclination angle on self-amplification action of a new adaptive wedge disc brake," *International Journal of Vehicle Performance*, vol. 2, no. 2, p. 166, 2016.

[23] M. H. Che Hasan, M. K. Hassan, F. Ahmad, and M. H. Marhaban, "A dynamic model of electronic wedge brake: experimental, control and optimization," *Indonesian Journal of Electrical Engineering and Computer Science*, vol. 23, no. 2, pp. 740–751, 2021.

[24] K. R. M. Mahmoud, M. Mourad, and A. Bin Mahfouz, "Dynamic behaviors of a wedge disc brake," *Applied Acoustics*, vol. 128, pp. 32–39, 2017.